UV-induced replication arrest in the xeroderma pigmentosum variant leads to DNA double-strand breaks, γ-H2AX formation, and Mre11 relocalization

Charles L. Limoli*†, Erich Giedzinski*, William M. Bonner‡, and James E. Cleaver§

*Department of Radiation Oncology, University of California, San Francisco, CA 94103-0806; ‡Laboratory of Molecular Pharmacology, National Institutes of Health, Bethesda, MD 20892; and §Department of Dermatology, Cancer Center, University of California, San Francisco, CA 94143-0808

Contributed by James E. Cleaver, November 15, 2001

UV-induced replication arrest in the xeroderma pigmentosum variant (XPV) but not in normal cells leads to an accumulation of the Mre11/Rad50/Nbs1 complex and phosphorylated histone H2AX (γ-H2AX) in large nuclear foci at sites of stalled replication forks. These complexes have been shown to signal the presence of DNA damage, in particular, double-strand breaks (DSBs). This finding suggests that UV damage leads to the formation of DSBs during the course of replication arrest. After UV irradiation, XPV cells showed a fluence-dependent increase in the yield of γ-H2AX foci that paralleled the production of Mre11 foci. The percentage of foci-positive cells increased rapidly (10–15%) up to fluences of 10 J·m^{-2} before saturating at higher fluences. Frequencies of γ-H2AX and Mre11 foci both reached maxima at 4 h after UV irradiation. This pattern contrasts sharply to the situation observed after x-irradiation, where peak levels of γ-H2AX foci were found to precede the formation of Mre11 foci by several hours. The nuclear distributions of γ-H2AX and Mre11 were found to colocalize spatially after UV- but not x-irradiation. UV-irradiated XPV cells showed a one-to-one correspondence between Mre11 and γ-H2AX foci-positive cells. These results show that XPV cells develop DNA DSBs during the course of UV-induced replication arrest. These UV-induced foci occur in cells that are unable to carry out efficient bypass replication of UV damage and may contribute to further genetic variation.

DNA damage | x-ray | S-phase | checkpoints | recombination

The S-phase checkpoint regulates DNA replication through a complex series of signaling events that ultimately coordinates the initiation of replicons and stabilization of replication forks with the detection and repair of DNA damage (1–3). Agents leading to the inhibition of replicon initiation or elongation can depress DNA synthesis until specific damage-responsive pathways can remove the brakes upon replication (4–6). UV light is one agent that leads to protracted replication arrest, particularly in the xeroderma pigmentosum variant (XPV; refs. 7–9). The replication deficiency observed in XPV cells is due to the absence of a functional bypass polymerase H (10, 11). In contrast to normal cells, which can efficiently replicate past UV-induced lesions, XPV cells experience extended arrest of the replication fork after UV exposure (12, 13). This arrest leads to relocalization of the Mre11/Rad50/Nbs1 recombination complex (Mre11 complex), a DNA-damage response that is not observed in normal cells (14). Mre11 was isolated originally in a meiotic recombination screen (15) and has multiple roles in the sensing, detection, and processing of DNA double-strand breaks (DSBs; refs. 16–18) and in the regulation of the S-phase cell-cycle checkpoint (19–21). The ability of repair-proficient cells to relocalize Mre11 in response to x- but not UV-irradiation suggests the Mre11 complex is recruited to sites of DSBs but not pyrimidine dimers. UV light does not directly produce DNA DSBs but rather produces pyrimidine dimers and other photoproducts, bulky adducts that must be removed or bypassed to prevent arrest of the replication fork (22). Therefore, the response of Mre11 to UV light in XPV cells suggests that UV-induced replication arrest leads to DSBs at or near stalled replication forks (14). UV-induced replication arrest in transformed XPV cells leads to marked increases in the level of sister chromatid exchanges (SCEs; ref. 23). Preferential use of the sister chromatid for homologous recombination (HR) of DSBs formed at stalled replication forks may explain these observations. Sister chromatid gene conversion has been reported to be a prominent pathway for the repair of DSB in mammalian cells (24, 25).

Inhibition of the *E. coli* replicative helicases Rep and DnaB has been shown to increase DSB levels, indicating that arrested forks are susceptible to breakage (26). Mutations in the RecQ family of helicases including the yeast SGS1 gene (27) and the gene mutated in Bloom's syndrome, BLM (28), produce similar hyperrecombination phenotypes. The ability of the BLM and WRN proteins to bind Holliday junctions (intermediates in HR) suggests that these helicases may prevent DSB formation by promoting branch migration to destabilize Holliday intermediates that arise inappropriately at stalled replication forks (29, 30). Elevated frequencies of SCEs characteristic of Bloom's syndrome have been observed in BLM-deficient chicken DT40 cells and are likely caused by HR of DSBs because simultaneous disruption of Rad54 eliminates this phenotype (31). Related data have shown that SCE levels are reduced significantly in DT40 cells lacking Rad51 and Rad54 (32). Cytostatic drugs have been reported to induce intrachromosomal recombination to varying extents in rodent cells (33), and similar work has found an increase in the level of HR when campthothecin was used to induce DSBs associated with replication forks (34). Mec1-dependent activation of Rad53 in yeast may protect against DSB formation during replication arrest by stabilizing stalled forks against collapse (35, 36). The activation of Chk2 by ataxia telangiectasia-mutated (ATM) and/or ataxia telangiectasia-related (ATR) in mammalian cells is an analogous pathway that has multiple roles in regulating S-phase progression in the presence of DNA damage (3, 37, 38). As opposed to lower organisms, the dependence of mammalian cells on signaling and recombinational repair enzymes for progression through S-phase suggests that DSB repair is essential for successful com-

Abbreviations: XPV, xeroderma pigmentosum variant; DSB, double-strand break; SCE, sister chromatid exchange; HR, homologous recombination; γ-H2AX, phosphorylated histone H2AX.

†To whom reprint requests should be addressed. E-mail: limoli@itsa.ucsf.edu.

The publication costs of this article were defrayed in part by page charge payment. This article must therefore be hereby marked "*advertisement*" in accordance with 18 U.S.C. §1734 solely to indicate this fact.

pletion of S-phase (related reviews may be found in refs. 66 and 67 and in other articles in those issues).

The identification of DSB-repair proteins at sites of arrested replication suggest that the inhibition of DNA replication leads to DSBs and recombination (14). Related work has shown that replication stress in mammalian cells leads to an ATR-dependent DNA-damage response involving phosphorylation of histone H2AX and BRCA1 (39). To determine the relationship between replication arrest, DSB production, and recombination in UV-irradiated XPV cells, changes in histone phosphorylation and Mre11 relocalization that depend upon DNA DSBs were monitored by immunofluorescence. DSBs lead to the rapid phosphorylation of histone H2AX yielding a modified phosphorylated histone H2AX (γ-H2AX; refs. 40 and 41). The specificity of this reaction provides a reliable marker for DSB production and the means to spatially localize DNA DSBs within the nuclei of cells (41). We report that UV-induced replication arrest in XPV cells is associated with the production of DNA DSBs and recombinational repair by the measurement of γ-H2AX and Mre11 foci.

Materials and Methods

Cell Culture. Simian virus 40 (SV40)-transformed human fibroblasts that exhibited a normal or replication-deficient UV-repair response were used in all studies. UV-repair-proficient cells permanently transformed by SV40 (GM637) were derived from the normal fibroblast cell line GM037. Replication-deficient cells permanently transformed with SV40 (XP30R0) were derived from the XPV fibroblast GM3617. The primary human fibroblast GM3617 contains a mutation in the XPV gene (*hRAD30A* or *POLH*) that leads to a chain termination of DNA polymerase H (10, 11). Each cell line was maintained in DMEM supplemented with 2 mM glutamine/100 units/ml penicillin/100 μg/ml streptomycin/10% (vol/vol) FBS (HyClone). Cells grown at 37°C in humidified incubators under 5% CO_2 exhibited doubling times in the range of 20–22 h.

X- and UV-Irradiation. Cultures of normal and XPV cells were maintained in exponential growth by routine passage twice weekly. One day before x- or UV-irradiation, 1×10^5 cells were seeded in dual-chambered slides (Nalge). Exponentially growing cells were exposed to either x-rays (Westinghouse Quadronex x-ray machine; 250 kVp, 15 mA, at a dose rate of 4.5 Gy/min) or UV light (254 nm at a fluence of 1.3 $W \cdot m^{-2}$) and were fixed 0.5–8 h after irradiation for 15 min in 2% (vol/vol) paraformaldehyde dissolved in 1× PBS. Slides containing fixed cells were air-dried and stored at −70°C until processing for immunofluorescence.

Immunofluorescence. Fixed cells were permeabilized in an ice-cold mixture of 50:50 acetone:methanol and allowed to come to room temperature. Cells were blocked for 1 h in 10% (vol/vol) FBS in 1× PBS at 37°C, rinsed, and incubated with primary antibody for 1 h at 37°C. Freeze-dried rabbit polyclonal serum against γ-H2AX (40, 41) was dissolved in water to 100 mg/ml and diluted 1:200. Rabbit polyclonal (Novus Biologicals, Littleton, CO) and Mouse monoclonal (GeneTex, San Antonio, TX) anti-hMre11 antibodies were diluted 1:200 or to 30 μg/ml, respectively. Secondary IgG (heavy and light chains) antibodies (Pierce) were selected to provide the appropriate combination of species specificity (goat-anti-rabbit or -mouse) and color discrimination (conjugated to either fluorescein or rhodamine). Secondary antibodies were diluted 1:200 and incubated with cells for 1 h at 37°C. Cells were counterstained with 0.1 μg/ml of 4′,6-diamidino-2-phenylindole (DAPI) in Vectashield (Vector Laboratories). All incubations were interspersed with three 5-min washes in 1× PBS, and all antibodies were diluted in 1× PBS in 1% BSA (including 0.5% Tween 20 for γ-H2AX). Antibody combinations required for colocalization experiments were incubated simultaneously.

Foci Quantification and Digital Image Analysis. Cell preparations were analyzed by using a Nikon Eclipse E600 fluorescent microscope equipped with a Spot RT Slider digital camera (Diagnostics Instruments, Sterling Heights, MI). Slides were scanned by eye at 630× magnification for the presence of γ-H2AX and Mre11 foci. Cells containing five or more foci per nucleus were scored as positive. A total of at least 500 nuclei were scored for each data point. Individual fluorochromes were visualized through a combination of single- and dual-bandpass filters for FITC, rhodamine, and DAPI. Single-color images were captured individually and merged electronically (by using manufacturer's Spot RT software) for the simultaneous visualization of multiple fluorophores.

Results

Formation of X-Ray and UV-Induced γ-H2AX Foci in XPV and Normal Cells. In the absence of DSBs, control cells show virtually no signal for γ-H2AX (Fig. 1*a*). DSBs produced by x-rays lead to the formation of nuclear γ-H2AX foci that can even be observed on the condensed chromosomes of XPV cells at various stages of mitosis (Fig. 1 *b* and *c*).

Other studies have shown that the Mre11 complex relocalizes in response to DNA DSBs, forming foci with a subset of these lesions during recombinational repair (16, 42). The induction of Mre11 foci coincident with proliferating cell nuclear antigen (PCNA) in UV-irradiated XPV cells suggested that DNA DSBs were formed during UV-induced replication arrest (14). XPV cells show large, UV-induced γ-H2AX foci that are clearly visible in the nuclei of irradiated (Fig. 1 *d–f*) but not unirradiated cells, thus demonstrating the presence of DSBs (Fig. 1*a*). Past (14) and present data collected from UV-arrested XPV cells support a role for the Mre11 complex in the repair of S-phase DSBs by HR (43).

Fluence Response for the Induction of γ-H2AX and Mre11 Foci in XPV and Normal Cells. To determine potential differences in the UV-damage response between XPV and normal cells, the formation of γ-H2AX and Mre11 foci was analyzed after exposing cells to increasing fluences of UV light. The number of XPV cells showing γ-H2AX and Mre11 (Fig. 2) foci increased up to ≈10 $J \cdot m^{-2}$ before saturating at higher UV fluences. Normal cells, on the other hand, exhibited a very low induction of either type of foci after UV exposure (Fig. 2). The fluence-dependent increases in γ-H2AX and Mre11 foci parallel one another closely and are much higher in XPV vs. normal cells (Fig. 2).

Kinetics of UV-Induced γ-H2AX and Mre11 Foci Formation in XPV and Normal Cells. To elucidate more completely the differences between XPV and normal cells in the UV-damage response, the kinetics of UV-induced γ-H2AX and Mre11 foci formation were investigated. The formation of UV-induced γ-H2AX (Fig. 3*A*) and Mre11 (Fig. 3) foci in XPV cells coincided over time. The yield of XPV cells showing both types of foci increased steadily after UV irradiation, reaching maximal levels (≈15%) 4 h later (Fig. 3). During this same postirradiation interval, very few foci-positive cells were observed in cultures of normal cells (Fig. 3). Figs. 2 and 3*a* reveal large differences between the responses of XPV and normal cells to UV light.

Kinetics of X-Ray-Induced γ-H2AX and Mre11 Foci Formation in XPV and Normal Cells. To determine whether similar differences would distinguish the x-ray damage response of XPV from normal cells, the kinetics of x-ray-induced γ-H2AX and Mre11 foci formation were analyzed. Cells given 6 Gy of x-rays were allowed to recover for various times before fixation and analysis of γ-H2AX and

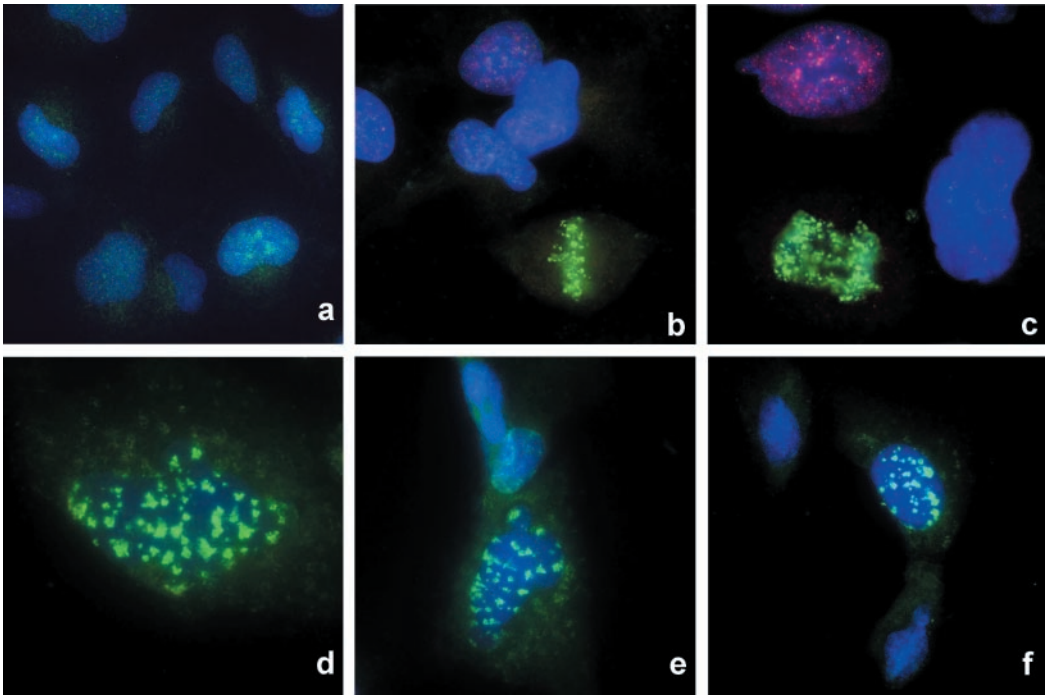

Fig. 1. X-ray- and UV-induced foci in XPV cells. (*a*) Unirradiated XPV cells showing the absence of foci. (*b* and *c*) X-ray-induced γ-H2AX foci on condensed metaphase (*b*) or anaphase (*c*) chromosomes in XPV cells fixed 30 min after 6 Gy of x-rays. (*d–f*) UV-induced γ-H2AX foci in XPV cells fixed 4 h after 13 $J \cdot m^{-2}$ of UV light.

Mre11 foci. Both normal and XPV cells showed a rapid increase in the yield of x-ray-induced γ-H2AX foci. The formation of x-ray-induced γ-H2AX foci peaked after 30 min before dropping sharply over the following 4 h (Fig. 3*B*). The formation of x-ray-induced Mre11 foci was more gradual. Maximal percentages of XPV and normal cells exhibiting large punctate Mre11 foci were not reached until 6–8 h after irradiation (Fig. 3*B*). Unlike the situation with UV light (Fig. 3*A*), XPV and normal cells exhibit similar temporal responses for the formation of γ-H2AX and Mre11 foci induced after x-irradiation (Fig. 3*B*).

Relocalization of γ-H2AX and Mre11 in XPV and Normal Cells After X-Irradiation. The disparity between the temporal response of x-ray-induced γ-H2AX and Mre11 foci suggests that not all DSBs that induce γ-H2AX formation lead to the recruitment of the Mre11 complex. This disparity also suggests that these two foci will coincide minimally in the nuclei of x-irradiated cells. To determine the spatial relationship of γ-H2AX and Mre11, cells were fixed 4 h after receiving 6 Gy of x-rays. This time corresponds to the maximum number of cells exhibiting both types of foci (i.e., the intersection of the plots shown in Fig. 3*B*). The data show that whereas cell nuclei contain both γ-H2AX and Mre11 foci, they exhibit little colocalization within the same cell nucleus (Fig. 4 *a–c*). Analogous experiments performed with normal cells revealed a similar pattern in the spatial relationship between γ-H2AX and the Mre11 complex.

Colocalization of γ-H2AX and Mre11 in XPV Cells After UV-Irradiation. The similarity in the fluence and temporal responses of γ-H2AX and Mre11 (Figs. 2 and 3*A*) suggest that in UV-irradiated XPV cells, replication arrest, DSB production, and Mre11 recombination are tightly linked in time and location. To determine whether γ-H2AX and Mre11 spatially coincide, cells were analyzed for the presence of foci 4 h after exposure to 13 $J \cdot m^{-2}$ of UV light, conditions that maximize the number of foci-positive cells. The images reveal that γ-H2AX and Mre11 foci colocalize in cell nuclei (Fig. 4 *d–i*), indicating a one-to-one correspondence between those cells showing γ-H2AX and those showing Mre11 foci. The colocalization of γ-H2AX and Mre11 foci in UV-irradiated XPV cells underscores yet another major difference in the UV-damage response between XPV and normal cells. The absence of these foci in UV-irradiated normal cells provides further support for the idea that replication arrest is responsible for eliciting the focal responses observed in UV-irradiated XPV cells.

Discussion

The absence of polymerase H in XPV cells disrupts translesion synthesis and leads to an extended S-phase delay as replication forks stall upon encountering UV-induced lesions (44). In UV-irradiated XPV cells, Mre11 foci form exclusively in replicating cells and colocalize with proliferating cell nuclear antigen (PCNA) bound in replication complexes (14). The association of the Mre11 complex at or nearby sites of stalled replication forks suggested that replication arrest also led to the development of DNA DSBs.

To test whether DSBs are produced by UV irradiation, we took advantage of recent reports documenting specific changes in histone phosphorylation in response to agents that produced DNA DSBs (40, 41). Histone H2AX is phosphorylated rapidly (within minutes) on Ser-139 to produce a specific modified form named γ-H2AX. By adapting a technique developed for producing DSBs in cells using visible light (45), γ-H2AX production was shown to depend on the production of DSBs, but not single-strand breaks (i.e., hydrogen peroxide does not elicit γ-H2AX, data not shown). γ-H2AX has since been used to monitor apoptosis (46), VDJ recombination (47), DNA damage (48), and synapsis in mice (49).

Our finding that UV light leads to γ-H2AX foci in XPV but not normal cells supports the idea that extended replication arrest leads to DSBs and provides an explanation for the marked differences in the temporal response between x-ray and UV-

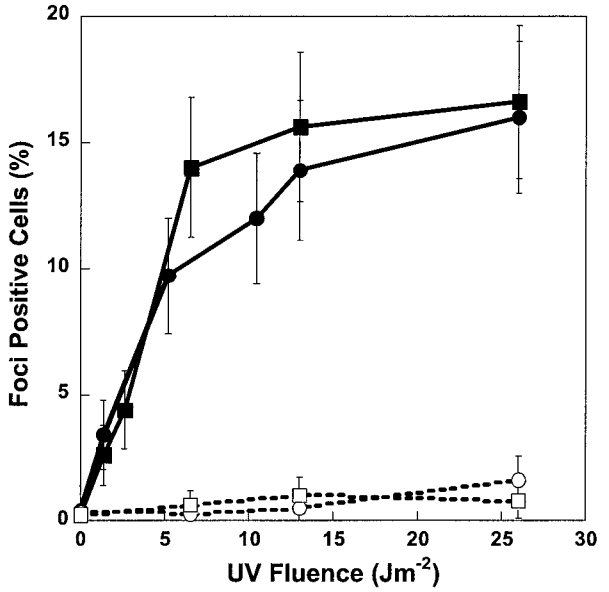

Fig. 2. Fluence response for the induction of Mre11 and γ-H2AX foci in XPV and normal cells. Cells subjected to a range of UV fluences (1.3–26 J·m^{-2}) were fixed 4–8 h after irradiation and analyzed to determine the percentage of foci-positive cells. Data showing the percentage of XPV (●) and normal (○) cells showing Mre11 foci are compared with data showing the percentage of XPV (■) and normal (□) cells showing γ-H2AX foci. The Mre11 data presented here are the same as those published (14) and are included for comparison. Data indicate that the production of Mre11 foci coincide with the production of DNA DSBs as detected by γ-H2AX foci. All data represent the average of three independent experiments and include error estimates expressed as ± SEP (standard error of the population).

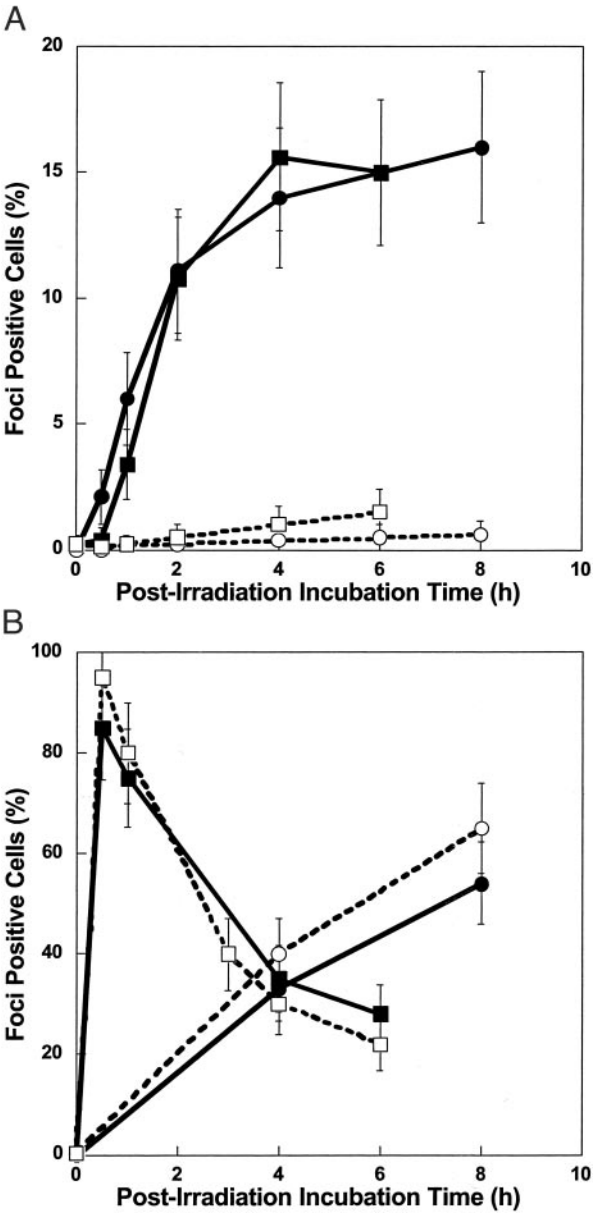

Fig. 3. Kinetics of UV- and x-ray-induced Mre11 and γ-H2AX foci formation in XPV and normal cells. Cells subjected to 13 J·m^{-2} of UV light (*A*) or 6 Gy of x-rays (*B*) were fixed at various times (0.5–8 h) after irradiation and analyzed to determine the percentage of foci-positive cells. Symbols are the same as in Fig. 2. Data indicate that the temporal production of UV-induced foci is similar, whereas that of the x-ray-induced foci is markedly distinct. All data represent the average of three independent experiments and include error estimates expressed as ± SEP.

induced foci. X-irradiation leads to a rapid increase in DSB levels that disappear over the course of a few hours (50). The induction and repair of these lesions is tracked by the formation and disappearance of γ-H2AX (41) and leads to the similarity between the x-ray damage response of XPV and normal cells. Therefore, Mre11 foci accumulate on a subset of x-ray-induced DSBs or on lesions that develop subsequently into suitable substrates. UV-irradiation, on the other hand, does not produce DSBs and γ-H2AX foci immediately. Rather, they accumulate more gradually over the duration of UV-induced replication arrest. Replication forks that arrest at sites of dimer impasse in XPV cells can collapse and develop into DSBs that elicit the formation of γ-H2AX. This fact leads to the striking difference in the UV response of XPV and normal cells and suggests that UV-induced replication arrest in XPV cells leads to the production of DSBs that recruit the Mre11 recombination complex. Our finding that UV light leads to equivalent yields of both γ-H2AX and Mre11 foci suggests the dependence of these responses on the production of DNA DSBs during replication arrest in XPV cells.

Colocalization provides a useful tool with which to probe the molecular interactions associated with replication arrest. The analysis of γ-H2AX foci allows one to pinpoint the spatial localization of DSBs formed in cells and whether DSBs are associated with specific types of repair complexes accumulating within the vicinity of stalled replication forks. Present and past colocalization data from UV-irradiated XPV cells demonstrate that DSBs are associated with Mre11 recombination complexes in the vicinity of stalled replication forks containing PCNA (14). The ability of the Mre11 complex to form a variety of nuclear-staining patterns in irradiated and unirradiated nuclei supports the involvement of this complex in the detection of exogenously and endogenously derived DNA damage (42).

The association of the Mre11 complex with DNA damage throughout the early and late stages of the DNA-repair process suggests this complex has multiple functions in the recognition and resolution of DNA DSBs (16, 17, 42, 48). Induction of DNA damage leads to the rapid activation of signaling kinases (ATM/ATR) (51–53), phosphorylation of H2AX and other substrates such as p53, NBS, Brca1, Chk2, etc. (41, 48), and poly(ADP-ribose) polymerase activation (54). DSB lesions then are recognized and, depending on their context, recruit specific repair factors. Although the details of subsequent events are unclear at present, binding of BRCA1 to sites of DNA damage may be instrumental in controlling the recombinational repair of

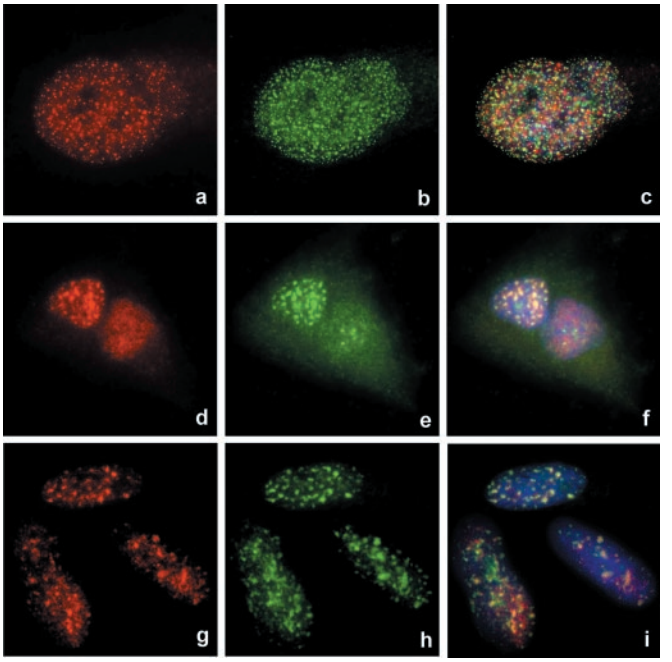

Fig. 4. Spatial localization of γ-H2AX and Mre11 in the nuclei of x- and UV-irradiated XPV cells. (*a–c*) X-ray-induced foci in XPV cells fixed 4 h after 6 Gy of x-rays. Rhodamine-labeled Mre11 foci (*a*), FITC-labeled γ-H2AX foci (*b*), and merged image of rhodamine and FITC signals showing lack of colocalization between Mre11 and γ-H2AX (*c*). (*d–i*) UV-induced foci in XPV cells fixed 4 h after 13 $J \cdot m^{-2}$ of UV light. Rhodamine-labeled Mre11 foci (*d* and *g*), FITC-labeled γ-H2AX foci (*e* and *h*), and merged image of rhodamine and FITC signals showing colocalization between Mre11 and γ-H2AX (*f* and *i*).

DSBs involving Rad51 and/or Mre11/Rad50/Nbs1 (55). Interactions between ATR, Chk2, p53, and BRCA1 may impose additional regulatory control over the concerted activities of DNA repair transpiring at stalled replication forks (3, 39, 53, 56).

The mechanisms of DSB formation at stalled forks in UV-arrested XPV cells are uncertain. Exposure of XPV cells to UV light produces lesions that block DNA synthesis on the leading strand of the replication fork, resulting in the progression of an asymmetrical fork that exposes large regions of single-stranded DNA (12, 13). These regions are then accessible to binding by replication protein A (or human ssDNA-binding protein), which is a substrate for several damage-responsive kinases able to modulate repair activity at sites of replication arrest (57, 58). Expanded regions of single-stranded DNA may possess damaged residues (sugar or base) or adopt structures (e.g., hairpins and triplex DNA) that lead to enzymatic nicking. The presence of inverted repeats within large single-stranded regions of an asymmetrical fork may facilitate formation of recombinogenic substrates and recruitment of the Mre11 complex. Inverted repeats have been shown to be hotspots for recombination (59, 60) and constitute the sequence motifs that can be driven by regions of microhomology to form hairpin and related structures recognized and cleaved by the Mre11 complex (61, 62). DSBs may then arise directly by nuclease activity, when the rebooted replication apparatus encounters other nicks in single-stranded regions, or when restart aborts and replication forks collapse (related reviews may be found in refs. 66 and 67 and in other articles in those issues).

The inability of cells to mount a normal repair response to DNA damage is a common theme relating a number of cancer predisposition syndromes. Ataxia telangiectasia, Nijmegen breakage syndrome, Bloom's syndrome, Fanconi's anemia, and XP all exhibit abnormalities in DNA repair, cell-cycle progression, and replication fidelity that lead to genomic instability and an increased risk of acquiring cancer (63, 64). The defects that characterize these specific disorders impact the ability of cells to tolerate DNA damage and execute the error-free duplication of DNA required to minimize mutation and maintain viability. Although major differences exist in the x-ray and UV-signal transduction pathways (e.g., ATM vs. ATR activation; refs. 3 and 65), replication arrest may reveal an overlap in these signaling pathways brought on by the breakdown of the replication fork and an accumulation of associated damage. The inability to mediate replication efficiently past UV-induced lesions leads to the inhibition of replication, the development of DNA DSBs and the activation of recombinational repair. The mechanisms by which cells respond to this stalled replication will dictate whether the ultimate fate of those cells is benign (recovery) or deleterious (carcinogenic). The recruitment of γ-H2AX and hMre11 to arrested replication forks represents a final recourse of cells that lack the bypass polymerase and are transformed (p53 deficient; refs. 14 and 23) and therefore may represent a mechanism of genetic instability present in many tumor cells. Understanding the details of these processes may provide clues to the underlying causes of carcinogenesis in human genetic diseases prone to dysfunctional DNA-repair responses after exposure to environmental carcinogens.

We thank the Xeroderma Pigmentosum Society, Poughkeepsie, NY, for their continued support and encouragement. This work was supported by American Cancer Society Grant RPG-00–036-01 CNE (to C.L.L.), National Institutes of Environmental Health Sciences Grant 1 RO1 ES 8061 (to J.E.C.), and an Ellison Senior Scholar Award (to J.E.C.).

1. Desany, B. A., Alcasabas, A. A., Bachant, J. B. & Elledge, S. J. (1998) *Genes Dev.* **12,** 2956–2970.
2. Schar, P. (2001) *Cell* **104,** 329–332.
3. Abraham, R. T. (2001) *Genes Dev.* **15,** 2177–2196.
4. Painter, R. B. & Young, B. R. (1975) *Radiat. Res.* **64,** 648–656.
5. Kaufmann, W. K. & Cleaver, J. E. (1981) *J. Mol. Biol.* **149,** 171–187.
6. Murnane, J. P. & Schwartz, J. L. (1993) *Nature (London)* **365,** 22–22.
7. Cleaver, J. E. (1972) *J. Invest. Dermatol.* **58,** 124–128.
8. Cleaver, J. E., Thomas, G. H. & Park, S. D. (1979) *Biochim. Biophys. Acta* **564,** 122–131.
9. Lehmann, A. R. (1979) *Nucleic Acids Res.* **7,** 1901–1912.
10. Johnson, R. E., Kondratick, C. M., Prakash, S. & Prakash, L. (1999) *Science* **285,** 263–265.
11. Masutani, C., Kusumoto, R., Yamada, A., Dohmae, N., Yokoi, M., Yuasa, M., Araki, M., Iwai, S., Takio, K. & Hanaoka, F. (1999) *Nature (London)* **399,** 700–704.
12. Cordeiro-Stone, M., Zaritskaya, L. S., Price, L. K. & Kaufmann, W. K. (1997) *J. Biol. Chem.* **272,** 13945–13954.
13. Cordeiro-Stone, M., Makhov, A. M., Zaritskaya, L. S. & Griffith, J. D. (1999) *J. Mol. Biol.* **289,** 1207–1218.
14. Limoli, C. L., Giedzinski, E., Morgan, W. F. & Cleaver, J. E. (2000) *Proc. Natl. Acad. Sci. USA* **97,** 7939–7946. (First Published June 20, 2000; 10.1073/pnas.130182897)
15. Petrini, J. H., Walsh, M. E., DiMare, C., Chen, X. N., Korenberg, J. R. & Weaver, D. T. (1995) *Genomics* **29,** 80–86.
16. Maser, R. S., Monsen, K. J., Nelms, B. E. & Petrini, J. H. J. (1997 *Mol. Cell. Biol.* **17,** 6087–6096.
17. Nelms, B. E., Maser, R. S., MacKay, J. F., Lagally, M. G. & Petrini, J. H. J. (1998) *Science* **280,** 590–592.
18. Carney, J. P., Maser, R. S., Olivares, H., Davis, E. M., Le Beau, M., Yates, J. R., 3rd, Hays, L., Morgan, W. F. & Petrini, J. H. (1998) *Cell* **93,** 477–486.
19. Lim, D. S., Kim, S. T., Xu, B., Maser, R. S., Lin, J. Y., Petrini, J. H. J. & Kastan, M. B. (2000) *Nature (London)* **404,** 613–617.
20. Wu, X. H., Ranganathan, V., Weisman, D. S., Heine, W. F., Ciccone, D. N., O'Neill, T. B., Crick, K. E., Pierce, K. A., Lane, W. S., Rathbum, G., *et al*. (2000) *Nature (London)* **405,** 477–482.
21. Zhao, S., Weng, Y. C., Yuan, S. S. F., Lin, Y. T., Hsu, H. C., Lin, S. C. J., Gerbino, E., Song, M. H., Zdzienicka, M. Z., Gatti, R. A., *et al*. (2000) *Nature (London)* **405,** 473–477.
22. Friedberg, E. C., Walker, G. & Siede, W. (1995) *DNA Repair and Mutagenesis* (Am. Soc. Microbiol., Washington, DC).

23. Cleaver, J. E., Afzal, V., Feeney, L., McDowell, M., Sadinski, W., Volpe, J. P. G., Busch, D. B., Coleman, D. M., Ziffer, D. W., Yu, Y. J., *et al*. (1999) *Cancer Res.* **59,** 1102–1108.
24. Elliott, B., Richardson, C., Winderbaum, J., Nickoloff, J. A. & Jasin, M. (1998) *Mol. Cell. Biol.* **18,** 93–101.
25. Johnson, R. D. & Jasin, M. (2000) *EMBO J.* **19,** 3398–3407.
26. Michel, B., Ehrlich, S. D. & Uzest, M. (1997) *EMBO J.* **16,** 430–438.
27. Watt, P. M., Hickson, I. D., Borts, R. H. & Louis, E. J. (1996) *Genetics* **144,** 935–945.
28. Ellis, N. A., Groden, J., Ye, T. Z., Straughen, J., Lennon, D. J., Ciocci, S., Proytcheva, M. & German, J. (1995) *Cell* **83,** 655–666.
29. Karow, J. K., Constantinou, A., Li, J. L., West, S. C. & Hickson, I. D. (2000) *Proc. Natl. Acad. Sci. USA* **97,** 6504–6508. (First Published May 23, 2000; 10.1073/pnas.100448097)
30. Constantinou, A., Tarsounas, M., Karow, J. K., Brosh, R. M., Bohr, V. A., Hickson, I. D. & West, S. C. (2000) *EMBO Rep*. **1,** 80–84.
31. Wang, W. S., Seki, M., Narita, Y., Sonoda, E., Takeda, S., Yamada, K., Masuko, T., Katada, T. & Enomoto, T. (2000) *EMBO J.* **19,** 3428–3435.
32. Sonoda, E., Sasaki, M. S., Morrison, C., Yamaguchi-Iwai, Y., Takata, M. & Takeda, S. (1999) *Mol. Cell. Biol.* **19,** 5166–5169.
33. Arnaudeau, C., Miranda, E. T., Jenssen, D. & Helleday, T. (2000) *Mutat. Res.* **461,** 221–228.
34. Arnaudeau, C., Lundin, C. & Helleday, T. (2001) *J. Mol. Biol.* **307,** 1235–1245.
35. Tercero, J. A. & Diffley, J. F. (2001) *Nature (London)* **412,** 553–557.
36. Lopes, M., Cotta-Ramusino, C., Pellicioli, A., Liberi, G., Plevani, P., Muzi-Falconi, M., Newlon, C. S. & Foiani, M. (2001) *Nature (London)* **412,** 557–561.
37. Hirao, A., Kong, Y. Y., Matsuoka, S., Wakeham, A., Ruland, J., Yoshida, H., Liu, D., Elledge, S. J. & Mak, T. W. (2000) *Science* **287,** 1824–1827.
38. Falck, J., Mailand, N., Syljuåsen, R. G., Bartek, J. & Lukas, J. (2001) *Nature (London)* **410,** 842–847.
39. Ward, I. M. & Chen, J. (October 22, 2001) *J. Biol. Chem.*, 10.1074/jbc.C100569200.
40. Rogakou, E. P., Pilch, D. R., Orr, A. H., Ivanova, V. S. & Bonner, W. M. (1998) *J. Biol. Chem.* **273,** 5858–5868.
41. Rogakou, E. P., Boon, C., Redon, C. & Bonner, W. M. (1999) *J. Cell Biol.* **146,** 905–916.
42. Mirzoeva, O. K. & Petrini, J. H. J. (2001) *Mol. Cell. Biol.* **21,** 281–288.
43. Yamaguchi-Iwai, Y., Sonoda, E., Sasaki, M. S., Morrison, C., Haraguchi, T., Hiraoka, Y., Yamashita, Y. M., Yagi, T., Takata, M., Price, C., *et al*. (1999) *EMBO J.* **18,** 6619–6629.
44. Cleaver, J. E. (1999) *Science* **285,** 212–213.
45. Limoli, C. L. & Ward, J. F. (1993) *Radiat. Res.* **134,** 160–169.
46. Rogakou, E. P., Nieves-Neira, W., Boon, C., Pommier, Y. & Bonner, W. M. (2000) *J. Biol. Chem.* **275,** 9390–9395.
47. Chen, H. T., Bhandoola, A., Difilippantonio, M. J., Zhu, J., Brown, M. J., Tai, X. G., Rogakou, E. P., Brotz, T. M., Bonner, W. M., Ried, T. & Nussenzweig, A. (2000) *Science* **290,** 1962–1964.
48. Paull, T. T., Rogakou, E. P., Yamazaki, V., Kirchgessner, C. U., Gellert, M. & Bonner, W. M. (2000) *Curr. Biol.* **10,** 886–895.
49. Mahadevaiah, S. K., Turner, J. M. A., Baudat, F., Rogakou, E. P., de Boer, P., Blanco-Rodriguez, J., Jasin, M., Keeney, S., Bonner, W. M. & Burgoyne, P. S. (2001) *Nat. Genet.* **27,** 271–276.
50. Ward, J. F., Limoli, C. L., Calabro-Jones, P. M. & Aguilera, J. (1991) *Radiat. Res.* **127,** 90–96.
51. Banin, S., Moyal, L., Shieh, S., Taya, Y., Anderson, C. W., Chessa, L., Smorodinsky, N. I., Prives, C., Reiss, Y., Shiloh, Y. & Ziv, Y. (1998) *Science* **281,** 1674–1677.
52. Canman, C. E., Lim, D. S., Cimprich, K. A., Taya, Y., Tamai, K., Sakaguchi, K., Appella, E., Kastan, M. B. & Siliciano, J. D. (1998) *Science* **281,** 1677–1679.
53. Tibbetts, R. S., Brumbaugh, K. M., Williams, J. M., Sarkaria, J. N., Cliby, W. A., Shieh, S. Y., Taya, Y., Prives, C. & Abraham, R. T. (1999) *Genes Dev.* **13,** 152–157.
54. De Murcia, J. M., Niedergang, C., Trucco, C., Ricoul, M., Dutrillaux, B., Mark, M., Oliver, F. J., Masson, M., Cierich, A., LeMeur, M., *et al*. (1997) *Proc. Natl. Acad. Sci. USA* **94,** 7303–7307.
55. Paull, T. T., Cortez, D., Bowers, B., Elledge, S. J. & Gellert, M. (2001) *Proc. Natl. Acad. Sci. USA* **98,** 6086–6091. (First Published May 15, 2001; 10.1073/pnas.111125998)
56. Tibbetts, R. S., Cortez, D., Brumbaugh, K. M., Scully, R., Livingston, D., Elledge, S. J. & Abraham, R. T. (2000) *Genes Dev.* **14,** 2989–3002.
57. Zernik-Kobak, M., Vasunia, K., Connelly, M., Anderson, C. W. & Dixon, K. (1997) *J. Biol. Chem.* **272,** 23896–23904.
58. Oakley, G. G., Loberg, L. I., Yao, J., Risinger, M. A., Yunker, R. L., Zernik-Kobak, M., Khanna, K. K., Lavin, M. F., Carty, M. P. & Dixon, K. (2001) *Mol. Biol. Cell* **12,** 1199–1213.
59. Gordenin, D. A., Lobachev, K. S., Degtyareva, N. P., Malkova, A. L., Perkins, E. & Resnick, M. A. (1993) *Mol. Cell. Biol.* **13,** 5315–5322.
60. Waldman, A. S., Tran, H., Goldsmith, E. C. & Resnick, M. A. (1999) *Genetics* **153,** 1873–1883.
61. Paull, T. T. & Gellert, M. (2000) *Proc. Natl. Acad. Sci. USA* **97,** 6409–6414. (First Published May 23, 2000; 10.1073/pnas.110144297)
62. Paull, T. T. & Gellert, M. (1998) *Mol. Cell* **1,** 969–979.
63. Fearon, E. R. (1997) *Nature (London)* **278,** 1043–1049.
64. Bootsma, D., Kraemer, K. H., Cleaver, J. E. & Hoeijmakers, J. H. J. (1998) in *The Genetic Basis of Human Cancer*, eds. Vogelstein, B. & Kinzler, K. W. (McGraw–Hill, New York), pp. 245–274.
65. Kim, S. T., Lim, D. S., Canman, C. E. & Kastan, M. B. (1999) *J. Biol. Chem.* **274,** 37538–37543.
66. Von Hippel, P. H., Kowalczykowski, S. C., Kreuzer, K. N., Michel, B., Egelman, E., Marians, K. J., Goodman, M. E., Flores-Rozas, H., Kolodner, R. D., Kass-Eisler, A., *et al*. (2000) *Trends Biochem. Sci.* **25,** 155–204.
67. Radding, C., Cox, M. M., Michel, B., Flores, M.-J., Viguera, E., Grompone, G., Seigneur, M., Bidnenko, V., Barre, F.-X., Soballe, B., *et al*. (2001) *Proc. Natl. Acad. Sci. USA* **98,** 8172–8468.